Mediterranean Aquaculture Journal 2024 11 (2): 15-35

Mediterranean Aquaculture Journal

https://maj.journals.ekb.eg

Print ISSN: 1687-7616 Online ISSN: 1687-7187

Original Article

A comprehensive study of histology and ultrastructure in the spine, tube feet, and aristotle's lantern of *Echinometra mathaei* from the northern Red Sea

Mohamed M. Rashad[1]*, Nesreen K. Ibrahim[2], Mohammed Salem[3], Saad Z. Mohamed[2], Hany A. Abdel-Salam[4]

[1] Department of Marine Ecology, Faculty of Aquaculture and Marine Fisheries, Arish University, Egypt
[2] Department of Marine Science, Faculty of Science, Suez Canal University, Ismallia, Egypt.
[3] Department of Marine Fisheries, Faculty of Aquaculture and Marine Fisheries, Arish University, Egypt
[4] Department of Zoology, Faculty of Science, Benha University, Benha, Egypt.

ABSTRACT

This study presents a detailed anatomical and histological investigation of the sea urchin *Echinometra mathaei*, emphasizing unique morphological structures and site-specific variations. In March 2023, echinoids were collected from two sites in the northern Red Sea at depths ranging from 0 to 5 meters. Various soft tissues, including the peritoneum, peristome, gills, podium, ampulla, and food canal, were extracted and preserved in 10% formalin. Sections of five microns were prepared and stained using the haematoxylin and eosin technique, followed by examination under a light microscope. The study concentrated on the external anatomy revealed distinct oral and aboral structures, including spines, pedicellariae, tube feet, and gills, with measurements indicating notable size and weight differences between specimens from the two collection sites. Internally, the digestive, nervous, and water vascular systems, as well as Aristotle's lantern and gonads, were described in detail. Histological analysis highlighted cellular arrangements in key structures such as the peristome, esophagus, stomach, and intestines, with unique features identified in connective tissues and epithelial layers. A key finding of this study is the observation of tricephalous pedicellariae, expanding the taxonomic understanding of *E. mathaei*. Morphological variations in tube feet ossicles between collection sites suggest environmental or genetic influences. Additionally, the ultrastructure of spines and stereom provided new insights into their composition and function. This comprehensive analysis enhances the knowledge of *E. mathaei*'s anatomy, contributes to echinoid systematics, and underscores its ecological adaptations across varying habitats.

Keywords: Burrowing sea urchin, *Echinometra mathaei*, Anatomy, Ultrastructure, Northern Red Sea.

1. INTRODUCTION

The phylum Echinodermata encompasses a diverse group of marine invertebrates that inhabit nearly all significant marine environments globally, ranging from intertidal zones to depths exceeding 5000 meters. Currently, echinoderms are classified into five classes: Crinoidea, Ophiuroidea, Asteroidea, Holothuroidea, and Echinoidea Echinoderms exhibit primary pentamerous symmetry in their adult forms, although they may also display secondary bilateral symmetry (Campbell, 1987).

Correspondence: Mohamed M. Rashad Mail: mohamed.rashad@aqua.aru.edu.eg
Department of Marine Ecology, Faculty of Aquaculture and Marine Fisheries, Arish University, Egypt
Received: Oct. 24, 2024 Revised: Nov. 16, 2024 Accepted: Nov. 21, 2024

A defining characteristic of all echinoderms is their mesodermal calcite skeleton. The distinctive spherical to oval calcareous test facilitates the differentiation between regular and irregular sea urchins (Zeina *et al*., 2016). Furthermore, echinoderms play a crucial role in marine ecosystems, influencing food web dynamics and substrate alteration (Zeina *et al*., 2016). Sea urchins are recognized as keystone species because they can influence the dynamics of algal resources through their grazing activities (Zeina *et al*., 2016). Echinoderms exhibit a diverse array of appendages associated with their test, including tube-feet, pedicellariae, sphaeridia, and spines. The tube-feet, composed of soft tissue, operate through hydraulic movement due to their connection to the internal water vascular system. Their primary roles encompass gas exchange and locomotion, as they can also function as suckers on various surfaces (Ruppert *et al*., 2004). Pedicellariae serve multiple purposes, including defense, feeding, and maintenance of cleanliness. Sphaeridia are present in the ambulacral areas of all echinoids, although they are absent in cidaroids (Cavey and Märkel, 1994).

Radial body symmetry is a key characteristic of the Echinodermata phylum, which arises from bilaterally symmetrical larvae that are free-swimming. The term "benthic form" applies to all adult forms within this phylum. Echinoderms are largely defined by their calcareous skeletons, external spines or knobs, and the presence of pentamerous radial symmetry. Additionally, they possess a multitude of tube feet that are hydraulically managed by a unique internal water vascular system. These tube feet play vital roles in locomotion, tactile feedback, excretion, and respiration, extending through the skeleton to interact with the external environment (Prabhu *et al*., 2015).

Sea urchins have a unique anatomical structure of ten pairs of plate-like structures, known as ossicles, arranged into five ambulacral and five interambulacral zones. The ambulacral plates have double pores corresponding to the tube feet, or podia. Each interambulacral plate features a tubercle that supports a primary spine. On the oral side, you'll find the mouth, called the peristome, while the anus, known as the periproct, is located on the opposite side. Sea urchins use the internal jaws of Aristotle's lantern to feed on a wide various of materials, such as debris, sponges, mussels, and algae. Their digestive system runs from the lantern to the anus, with the internal cavity filled with fluid and gonads (Großmann, 2010).

Echinoid spines serve multiple purposes, including defense due to their spiky and somewhat toxic nature, aiding in burrowing, reducing wave energy, and assisting in movement (Cavey and Märkel, 1994).

Strathmann (1981) discusses how these spines protect against structural damage. A closer look reveals that the spine consists of two primary sections: the base, which can have either a perforated or non-perforated acetabulum, and the shaft, that includes the neck and tip (Märkel and Röser, 1983). The junction between the base and shaft features a distinct element known as the milled ring. Additionally, the structural aspects of spines can help in taxonomic classification, as the shaft may vary in appearance from smooth to decorated with thorns, granules, and ribs. Primary spines are notably larger than the adjacent secondary spines, while miliary spines, which are the tertiary spines, are used for cleaning the test surface (Großmann, 2010).

Due to the lack of extensive studies on the Red Sea sea urchin, *E. mathaei*, this research aims to explore its anatomy, examine the ultrastructural features of its spines and Aristotle's lantern, and analyze the histological makeup of specific compartments.

2. MATERIALS AND METHODS

2.1. Sample collection

Five specimens of *E. mathaei* from each study site, weighing between 50 and 90 grams, were manually collected from coastal waters at depths ranging from 0.5 to 3 meters in Al Ain Al Sukhna and

Hurghada, located in the northern Red Sea. The collection took place in March 2023, with coordinates of (29° 33' 20.7" N & 32° 21' 44.8" E) for Al Ain Al Sukhna and (27° 17' 07.5" N & 33° 46' 11.8" E) for Hurghada.

The specimens were maintained in a living state and sent to the marine genomics laboratory at the Faculty of Science, Benha University, where they were examined and photographed. Their genus and species were identified based on morphological characteristics outlined by (Zeina *et al*., 2016).

2.2. Anatomy

The examination of the specimen's anatomy involved a comprehensive analysis of its general characteristics, including its shape, size, color, spines, tube feet, and shell composition. The external morphology was categorized into oral and aboral regions.

The oral perspective focused on the mouth and associated structures, such as the teeth, peristome, gills and pedicellariae. In contrast, the aboral view covered the anus, madreporite, and gonopores, along with the genital plate and foramen. Before examining the internal organs, the specimens were carefully chilled on ice for 45 minutes.

The internal examination included assessing the coelomic cavity, digestive tract, Aristotle's lantern, ampulla, gonads, and the peritoneal epithelium. All findings were carefully documented using a digital camera (Canon).

2.3. Preparation of spine, tube feet and Aristotle's lantern for Scanning electron microscope investigation:

Following the dissection of the species, which involved the separation of the spine, tube feet, and Aristotle's lantern, the samples were preserved by immediate fixation in a solution comprising 4% formaldehyde and 1% glutaraldehyde (4F1G) in a phosphate buffer (pH 7.2) at 4°C for three hours. The dissected parts underwent washing in the buffer and were subsequently dehydrated at 4°C through a series of graded ethanol concentrations. The specimens were then post-fixed in a 2% osmium tetroxide (OSO4) solution within the same buffer at 4°C for two hours, followed by additional washing in the buffer solution, dehydration at 4°C through graded ethanol, and drying via the critical point method utilizing a Tousimis Samdri-795 apparatus. The samples were then mounted on aluminum stubs, coated with a gold/palladium layer of 5–8 nm thickness using a Hummer 6.2 sputter coater, and examined with a JEOL JSM-5300 Scanning Electron Microscope (SEM) operating at 15 to 20 keV (Rashad *et al*., 2020).

2.4. Histology

The internal organs, which include the epithelium, tube feet, ampulla, digestive system, and peristome, were dissected and subsequently fixed in buffered formalin (10%, pH = 7) provided by Sigma Co. in Germany. Following a 48-hour fixation period, the tissue samples underwent processing in an automated tissue processor and then embedded in paraffin wax. Sections measuring 4–5 μm thickness were prepared and stained using haematoxylin and eosin stain.

3. RESULTS

3.1. Taxonomy of Echinometra mathaei (Blainville, 1825):

The position of this genus at the taxonomic level is presented in (Table 1)

Table 1: Classification of *E. mathaei.*

Kingdom:	Animalia
Phylum:	Echinodermata
Class:	Echinoidea
Order:	Echinoida
Family:	Echinometridae
Genus:	*Echinometra*
Species:	*Echinometra mathaei*

*3.2.**External anatomy of E. mathaei:***

The external anatomy of *E. mathaei* specimens is divided into oral and aboral poles. Observations showed features such as the peristome, tube feet, spines, pedicellariae, and gills. The shell of *E. mathaei* was typically oval to spherical and exhibited a dark red or brown coloration. The Specimens from the first collection site (Al Ain Al Sukhna) measured between 26 and 61 mm, while those from the second site (Hurghada) ranged from 44.5 to 131 mm in diameter. The average weight of the specimens from the first site was 35 ± 6.095 g, whereas the average weight for those from the second site was 86.74 ± 18.46 g.

3.2.1. Oral view of E. mathaei shell:

Four major compartments had been seen in the oral view: the peristome, mouth, teeth, and gills. The oral view of *E. mathaei* individuals was the same at the two study sites (Figure 1).

Peristome and mouth:

The peristome featured a red outer layer that lacked spines, as shown in Figure 2A, which also displayed a few small pedicellariae scattered on its surface. These pedicellariae appeared as small to medium rods with thicker heads resembling closed forks. The mouth was located next to an inner, dark brown layer densely populated with tiny pedicellariae (Figure 2 B).

Arranged around the edge of this inner peristome layer were five pairs of small oral tube feet, referred to as buccal tube feet (podia), arranged in a circle (Figure 2 A). These tube feet were distinct from the others due to their thicker and smaller construction.

In the center of the lower oral view, the mouth featured five teeth (Figure 2 B) surrounded by a soft, collar-like lip. Beneath each tooth were five pink, diaphragm-like tissues (Figure 2 B).

A circular dark red line bordered several overlapping conical tissues, which appeared pink to red when the mouth was either partially or fully closed (Figure 2 B). It was suggested that the five pairs of short, thick tube feet at the mouth's edge helped prevent food from sticking too firmly, allowing the teeth to manipulate it more effectively.

It was observed that the five teeth could rotate in various directions, a flexibility attributed to the connective tissue within the peristome. Additionally, it was noted that the peristome could elongate centrally to cover the teeth, effectively closing the mouth cavity**.**

Spines:

Spines serve various purposes, such as burrowing, reducing wave impact, facilitating movement, and providing protection, often being spiky and sometimes partially toxic.

Upon close inspection, a spine can be divided into two main sections: the shaft, which consists of the neck and the tip, and the base, which can feature either an imperforate or perforate acetabulum. The milling ring is a raised area that marks the division between the base and the shaft (Figure 3 & 4). The diverse shapes of a spine's shaft can also aid in taxonomic classification. The shaft may be smooth or adorned with ribs, grains, and thorns. Primary spines are larger than the surrounding secondary spines, while the smaller tertiary spines, known as miliary spines, also help remove debris from the test surface. A ball-and-socket joint connects the spines to the sea urchin's skeleton (Figure 4). The catch apparatus, a circular ligament, enables the spine to maintain a specific position if threatened by predators or in other circumstances. Muscles and nerves (collagen bundles) link the test to the tubercle, allowing spine manipulation. These collagen bundles can be organized into 30-micron strands.

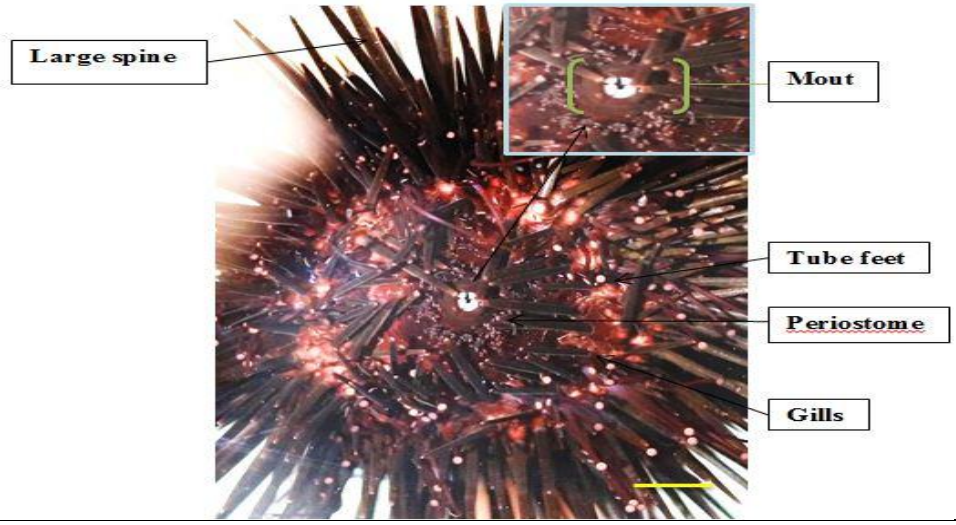

Figure 1: The photograph presents an oral view of the Red Sea sea urchin, *Echinometra mathaei*, collected from the first location (Al Ain Al Sukhna). The image illustrates the external features. Scale bar = 5 mm

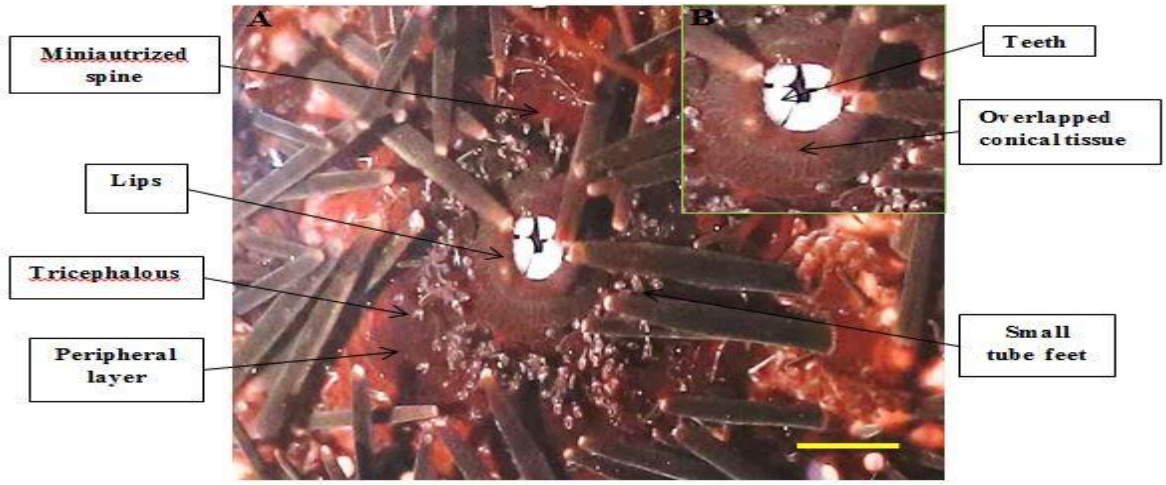

Figure 2: A photograph Oral view of sea urchin, *E. mathaei* demonstrates the peristome. (A) The area surrounding a sea urchin's mouth known as the peristome was covered in pedicellariae, tube feet, and spines. As well as five sets of tiny tube feet. (B) Five diaphragm-like tissues encircled the mouth's five teeth. Scale bar = 1mm

The medulla, which runs cylindrical from the base to the tip, is located in the center of the spine and is surrounded by a radiating layer (Figure 5), that transitions into the outer growing ring, known as cidaroids, associated with the Echinoida family.

When examining the spine, various stereom distribution morphologies are evident, ranging from denser forms as seen in *E. mathaei*. The growth rings of *E. mathaei* segment its spine, distinguishing it from the innermost area, the medulla, and the radiating layer (Figure 5).

Ultra-structure of *E. mathaei* spine:

The microstructure of the spines, referred to as the stereom, features a porous three-dimensional configuration composed of trabeculae (or struts) (Figure 6 A). The spaces within this structure, known as stroma, are occupied by fluid,

connective tissue cells, and extracellular fibers. The predominant cell type in the stereom is sclerocytes, which are tasked with generating the skeleton. The stereom of *E. mathaei* spines exhibits micro-perforation characterized by irregular perforations in the calcite layer and upright canals (Figure 6 B). The ultrastructure of the spines reveals that they are made up of solid plates interconnected by trabeculae (Figure 6 C). Additionally, the spicules, which vary by species, are also notable. Figure 6 D illustrates that the spicules of *E. mathaei* have a semi-circular shape.

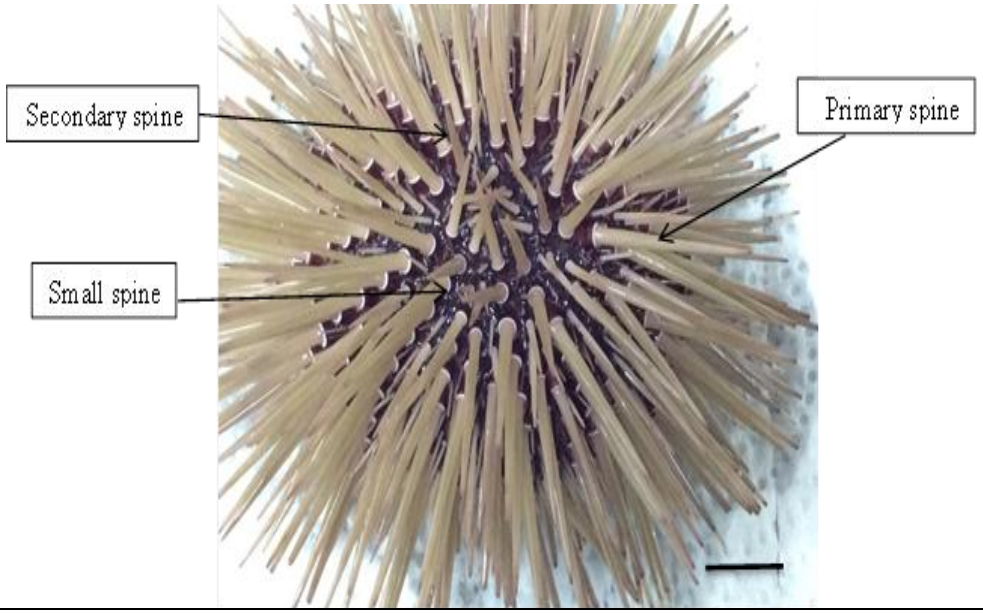

Figure 3: A photographed image of aboral view shows the primary and secondary spines of *E. mathaei* in addition to the small spines. Scale bar = 10 mm.

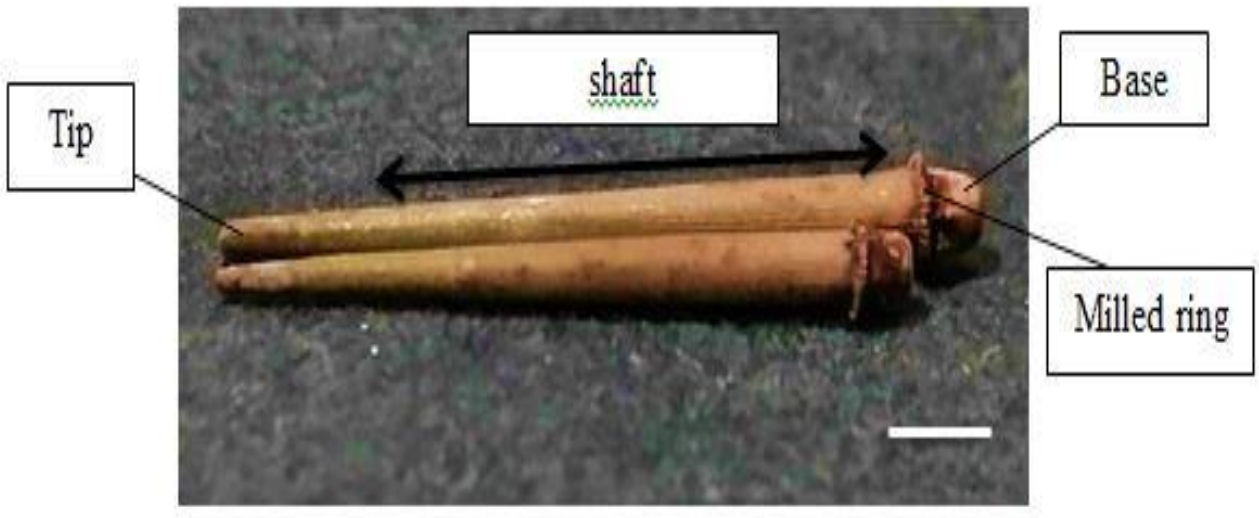

Figure 4: *Echinometra mathaei* primary spines. scale bar = 5 mm.

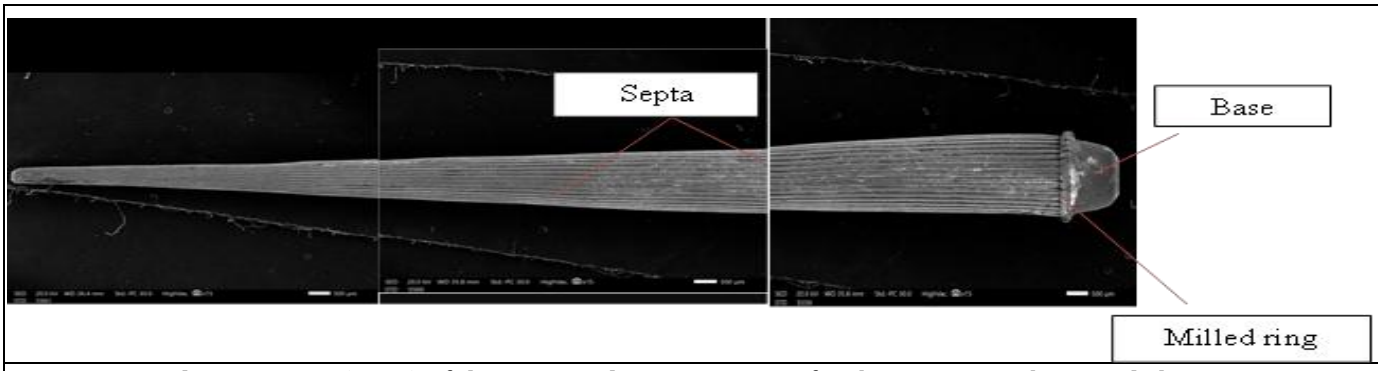

Figure 5: Ultra-structure (SEM) of the examined primary spine of *Echinometra mathaei*. scale bar = 500 µm

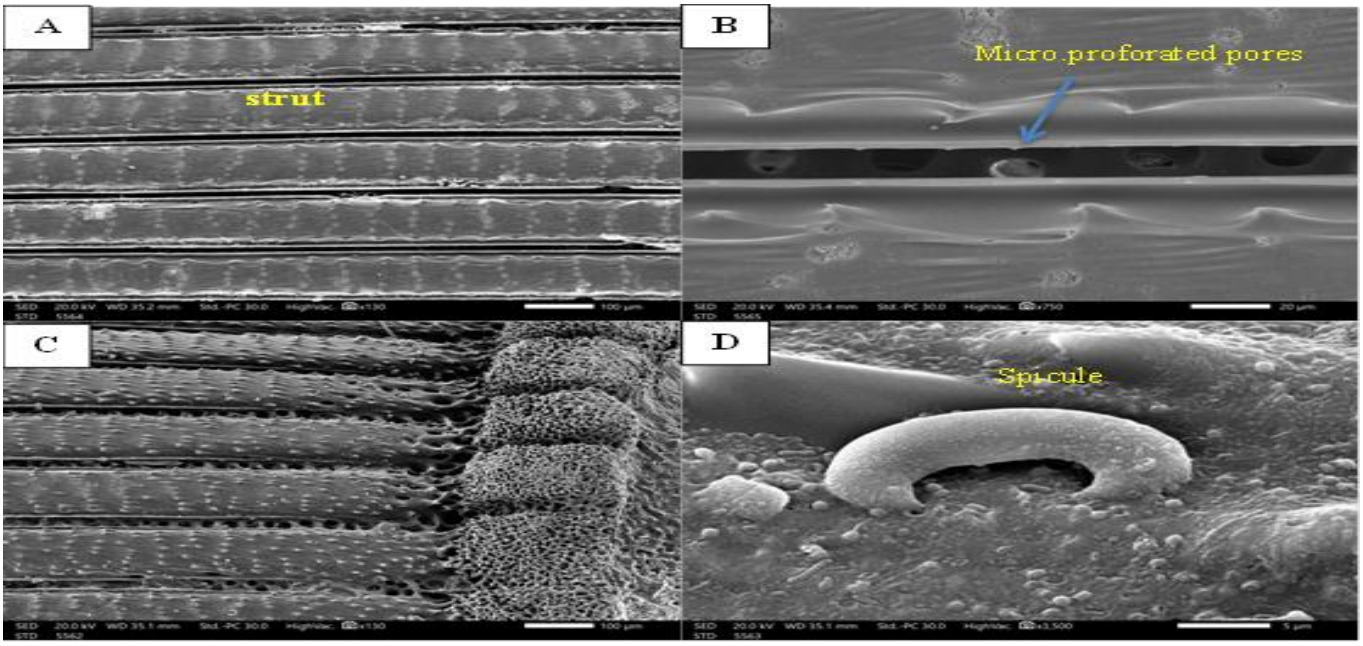

Figure 6: Ultra-structure of *Echinometra mathaei* primary spine under Scanning Electron Microscope (SEM). (A) the struts (plate) arrangement of the spine, (B) shows the connection between theplate through microperforated cortex, (C) illustrates the base of the spine and the white ring structure, which is characterized of *E. mathaei*. nd (D) shows the spicule type in *E. mathaei.* Scale bar (A &C = 100 µm, B = 20 µm, and D = 5 µm).

Pedicellariae:

There are five types of pedicellariae: small tridentate, large tridentate, trifoliate (triphyllous), tricephalous, and globiferous.

Our research team has observed the tricephalous pedicellariae. These structures were found on the spines and tube feet on both the oral and aboral sides (Figure 7).

Gills:

The peristome was surrounded by five pairs of gills that resembled undulating white masses. Figures 1 and 7 clarify that each had multiple primary branches, with supplementary branches protruding to the surface.

Tube Feet:

Three types of tube feet were observed: two large types and one small type. The two large tube feet

were arranged in five rows when viewed from both the oral and aboral sides, and were classified into two categories: oral and aboral.

The oral tube foot consisted of a short cylindrical tube (stem) (Figures 8 A, 9 A, 10 A & 11 A) that connected to a larger, discus-shaped head (distal disc) (Figures 8 A, B, 9 A, B, 10 B & 11 B).

It was white and featured a small central opening. There was also a slight groove extending from the shell to the head.

Additionally, the oral tube foot had a narrower cylindrical section that ended in a smaller discus head, which also had a similar bilateral groove. Small tube feet were discovered in the mouth, positioned between the pedicellariae.

These tube feet resembled the larger ones, but they had distinct features: a light red discus head and a sturdy, dark brown body.

There were ten small tube feet in total, arranged in pairs to form a circle around the mouth cavity (Figures 1 and 7). The distinctive hydraulic structures known as tube feet are present in all echinoderms and play crucial roles in respiration, light sensitivity, chemoreception, and movement.

In the case of *E. mathaei*, five ossicles are arranged at the distal end of the tube foot, acting as light collectors with their concave surfaces facing the light source (Figures 8 C & 9 C). These ossicles are lined with color cells and contain perforations (Figures 8 C, 9 B, 10 C & 11 C).

There was a noticeable change in the morphology of the ossicles between the two research sites. At the first site, the ossicles of *E. mathaei* exhibited five irregularly shaped perforations (Figure 8 B). In contrast, the ossicles collected from the second site in Hurghada displayed five uniformly shaped perforations, with solid sections between the pores and multiple layers of ossicles (Figure 9 C).

The duo-gland adhesive system located in the distal plate of the tube foot epidermis produces both sticky and de-adhesive substances.The adhesive secretions create a thin layer that helps the tube foot attach to surfaces, while the de-adhesive secretions enable detachment, often leaving a mark behind.

The semi-circular spicules found in the tube foot of *E. mathaei* from the two research sites are illustrated in (Figures 8 D and 9 D).

Sea urchins can perceive low light, mainly in the green spectrum, which helps regulate gametogenesis through photoperiods. They detect changes in their environment's light and adjust their physiological processes and behaviors using their tube feet.

Figures 10 & 11 show the tube feet structure of *E. mathaei* from two study sites.

The ultrastructure of the distal disc epidermis in tube feet features numerous micro-projections that enhance adherence to surfaces (Figures 10 D & 11 D).

In *E. mathaei*, the diameter of the distal disc from the outer point of the ossicles ranges from 662 µm to 705.3 µm, and from the inner peripheral part, it spans 536.2 µm to 593.2 µm at the first site. At the second site, the outer diameter ranges from 527.8 µm to 679.1 µm, and the inner diameter from 393.9 µm to 525.3 µm.

*3.2.2. **Aboral view***

The aboral perspective showed a shape that was either spherical or oval, featuring tube feet, spines, pedicellariae, a madreporite, genital plate, ocular plate, and anus (Figure 12 A).

Test (shell)

The test appeared as an oval-shaped, light green hemisphere. Tube feet have five pairs of pores in a row that form a semi-circle between two spines. Figure 12 shows that one pore in each tubercle of two spines was larger than the others. Tiny spines encircled the anus, as shown in Figures 12 A & B. Tube feet were arranged in five radial rows in pairs (Figure 12 A). Figure 3 shows a distribution of large spines in five radial pairs adjacent to tube foot rows.

Figure 7: A photograph illustrates the pericellariae, Tube feet and gills in *E. mathaei* species. Scale bar = 1 mm.

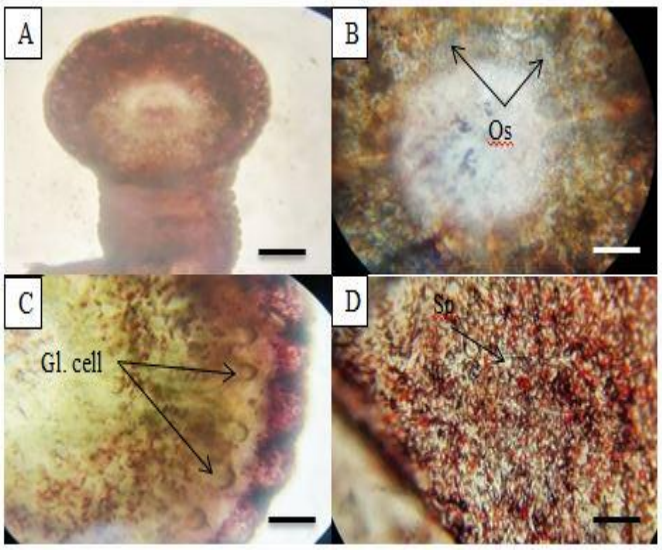

Figure 8: Micrograph shows the tube feet (podia) of *E. mathaei* from the first study site (El-Ain El-Sukhna, Red Sea, Egypt). (A) show the distal disc, (B) Show the five ossicles that are irregularly perforated, (C) show the distal disc epidermis which contains glands for both adhesive and de-adhesive material and pigmented cells and (D) show the kind of spicules which present in tube feet stem. Abbr. Os, Ossicles; Gl. Cell, Glandular cell and Sp, Spicules. Scale bar (A= 1mm, B &C =500µm and D= 200 µm).

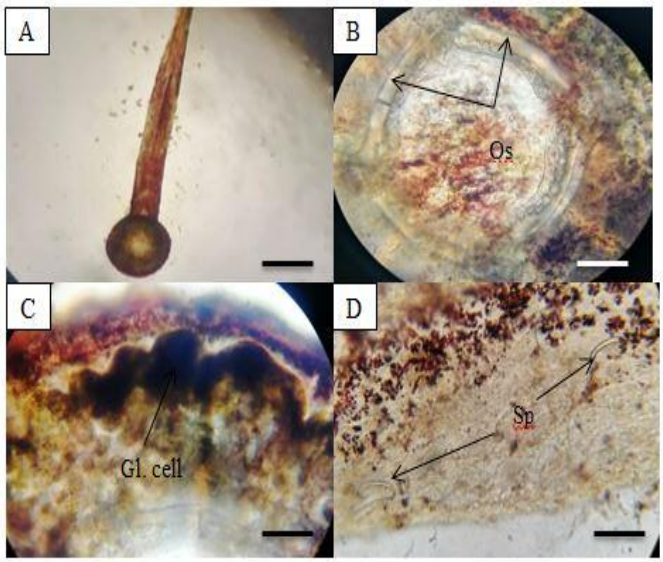

Figure 9: Micrograph shows the tube feet (podia) of *E. mathaei* from the second study site (Hurghada, Red Sea, Egypt). (A) show the distal disc, (B) Show the five ossicles, Which are totally irregular and perforated, (C) show the distal disc epidermis, which contains glands for both adhesive and de-adhesive material and pigmented cells and (D) show the kind of spicules which present in tube feet stem. Abbr. Os, Ossicles; Gl. Cell , Glandular cell and Sp, Spicules. Scale bar (A= 1 mm, B &C =500 µm and D= 200 µm).

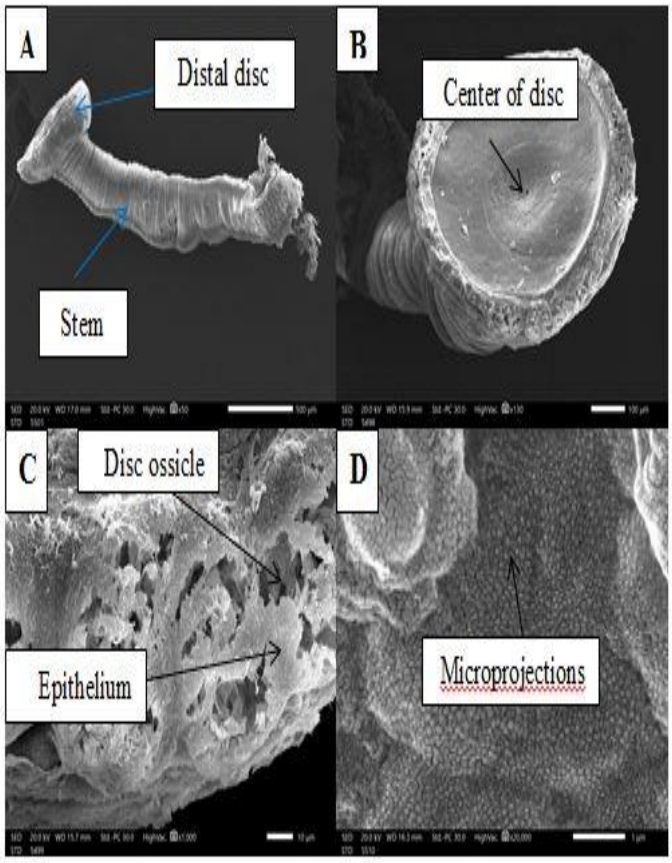

Figure 10: Scanning Electron Microscope images of Tube feet (podia) of *E. mathaei* from the first study site (El-Ain El-Sukhna, Red Sea, Egypt). (A) shows the distal disc and stem, (B) Shows the center of the distal disc which consists of five ossicles, (C) shows the distal disc epidermis and ossicles, and (D) shows the micro-projections in tube feet which increase the adhesive of the tube feet with substratum. Scale bar (A= 500 µm, B= 100 µm, C=10 µm and D= 1 µm).

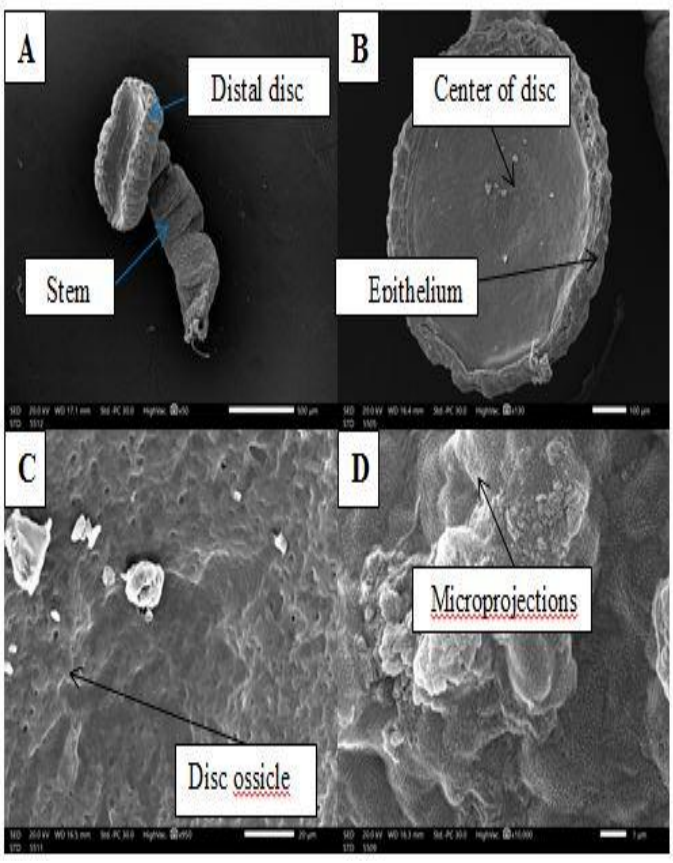

Figure 11: Scanning Electron Microscope images of tube feet (podia) of *E. mathaei* from the second study site (Hurghada, Red Sea, Egypt). (A) shows the distal disc and stem, (B) shows the center of the distal disc, which consists of five ossicles and the distal disc epidermis (C) shows the distal disc ossicles, and (D) shows the micro-projections in tube feet, which increase the adhesive of the tube feet with substratum. Scale bar (A= 500 µm, B= 100 µm, C= 20 µm and D= 1 µm)

Spines of various sizes were found in the center and edges of the anus, including medium, little, micro, and tinny. The middle region of the aboral view showed a periproct plate covered with small spines. The anus openning was placed in the center of the periproct, surrounded by microscopic and mini-spines. Figure 12 B shows five ocular and five genital plates arranged in a triangle, with apical ocular and genital pores.

Internal anatomy:

From an internal perspective, the features of the mouth skeleton (lantern), the peritoneal membrane and cavity, the nervous system, the water vascular system, the gonads, and the digestive system are described.

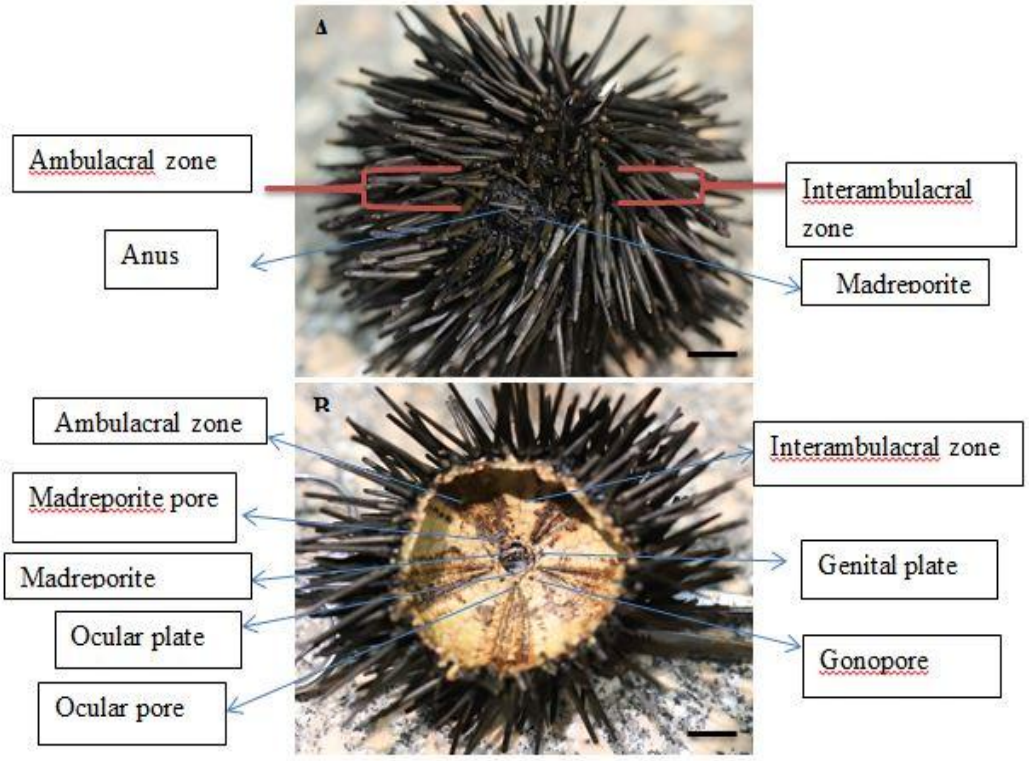

Figure 12: *Echinometra mathaei* Aboral view. A. This specimen features ten meridional rows of tube feet, or podia, extending from the oral to aboral poles. These rows beautifully form five distinct ambulacra, each consisting of two tube feet. Notably, the ambulacra are divided by inter-ambulacral zones, lacking tube feet. B. At the aboral pole, the periproct is a small, yet significant area encircling the anus. Scale bar (A&B = 10 mm).

Digestive system:

There were five primary components to the digestive system: the mouth, esophagus, stomach, intestine, and anus (Figure 13).

Aristotle's lantern's center was traversed by an esophagus that emerged from the mouth. The esophagus widened and twisted in the direction of the stomach. The stomach formed a circle inside the test on the peri-visceral coelom floor. The gut had the size of a large bag. Mesenteries were used to link the digestive system to the test walls (Figure 13).

The nervous system

The nervous system has a straightforward structure, although the neural ring can be difficult to see during dissections. Encircling the mouth is a large nerve ring located within the lantern. From this nerve ring, five nerves branch out into the radial canals of the water vascular system (Figure 13).

Peritoneum (Peritoneal membrane):

The peritoneum was adjacent to all internal organs, including the gonads, digestive system, and Aristotle systems, and filled with a liquid known as coelomic fluid. The outer and inner layers of the peritoneum were close to the internal skeleton and coelomic fluid, respectively. (Figures 13 and 14).

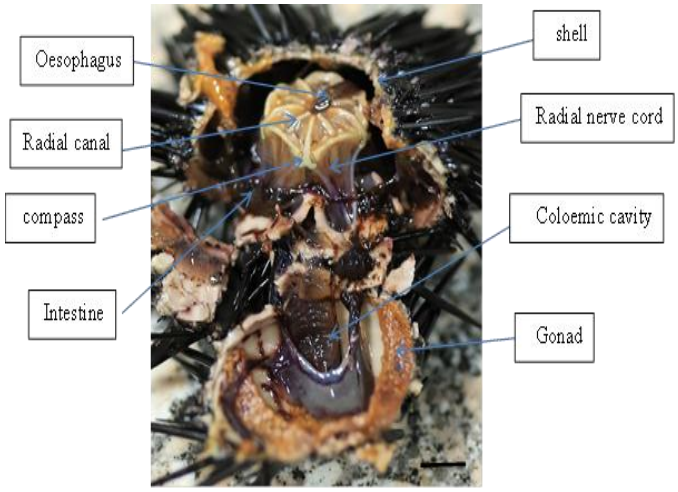

Figure 13: Photograph of dissected *E. mathaei* illustrates the digestive and nervous systems. The internal organs are situated within the peritoneal cavity, separated by the peritoneal membrane, which also encases the gonads. The esophagus begins at the aboral end of the lantern and extends to the stomach. The intestines are represented as bulging structures within the peritoneal cavity, connected to the internal skeleton by various ligaments. The scale bar = 10 mm.

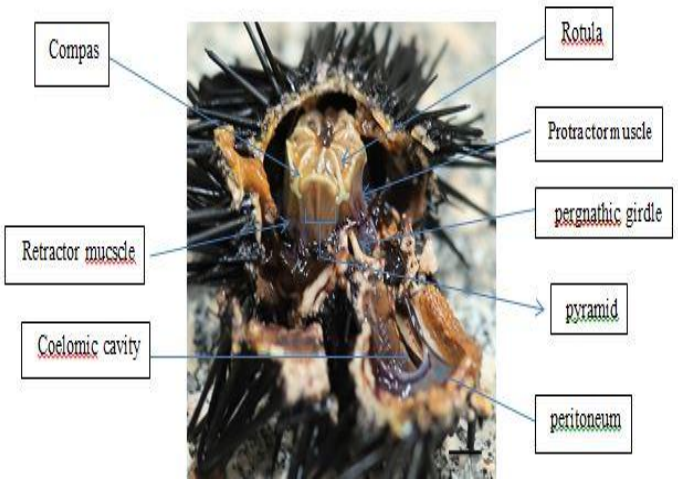

Figure 14: Photograph of dissected *E. mathaei* shows the internal organs and the Arisotle's lantern. From the oral to the aboral end, the lantern was longer. It led to a pyramidal portion in this view, from which five teeth are visible. Axial examination revealed five curving forks extending from the lateral body to the ring canal. There were five radial canals, encircled by peripharengial coelom, situated in between those curving forks. The reproductive system is situated on the outside of the cavity, which ends in five gonopores when viewed in an anterior perspective, and is full of yellow-golden gonads. Scale bar = 10 mm.

Aristotle's lantern:

After the remaining digestive tract was removed, Aristotle's lantern became visible. This intricate structure, known as Aristotle's lantern, is composed of both soft and hard tissues. It is located in the center of the test, with one part extending toward the esophagus that surrounds the pharynx and another leading to the mouth beneath the peristome. The peripharyngeal peritoneum encircles the lantern, and each tooth is surrounded by a dental sac formed from this peritoneum. Aristotle's lantern consists of five ossicles, each associated with muscles. These bone-like structures have a pyramidal shape and support the teeth, functioning like "jaws." The lantern is also equipped with five pieces called rotulas (Figure 14), which connect to the pyramids via protractor and retractor muscles. These muscles allow for the extension and flexion of the lantern. A bony structure known as the "perignathic girdle" extends from the test into the internal space (Figure 14). Among the muscle groups, the girdle connects the test to the lantern.

The lantern is operated by four specific muscle groups: protractors, retractors, interpyramidals, and compass elevators. The protractor muscles link the upper surface of the pyramids to the perignathic girdle, while the retractor muscles extend from the internal oral pole of the pyramid to the auricles (Figures 14 & 15).

The variations in the morphology of the urchin's oral apparatus play a crucial role in the systematics of this group, particularly in the macro- and microstructure of the teeth. The jaw structure, known as Aristotle's lantern, exhibits five-fold symmetry, with each section comprising a single tooth (Figure 15).

These teeth are held to the pyramidal structure by collagenous tissue at a part referred to as the dental slide. They are only supported across part of their length and extend beyond the dental slide as curved cantilevers (Figure 15 B). With the exception of sand dollars, sea urchin teeth are typically long and narrow.

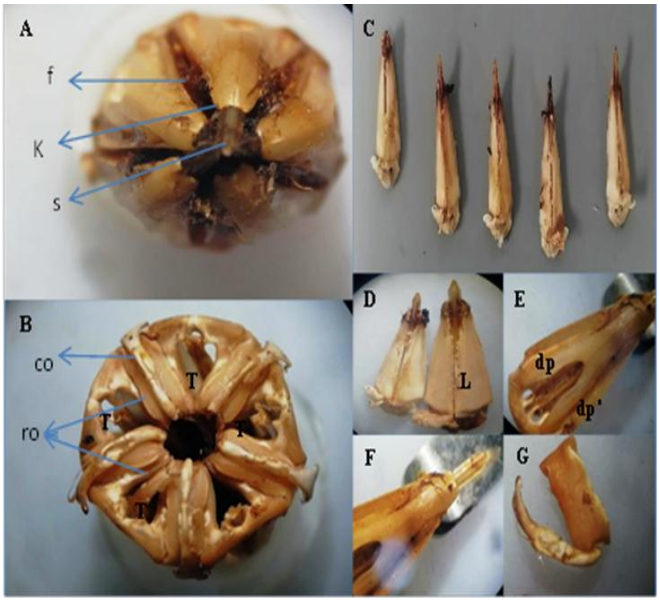

Figure 15: Aristotle lantern of *E. mathaei* under the dissecting microscope. A; shows the pentagonal arrangement of the five teeth, B; showing the downside of Aristotle lantern and the five teeth with the structure that was connected to muscles responsible for opening and moving the Aristotle lantern in all directions. C; showing the five teeth after they dissected and separated from each other's, D; show the lamella structure of the teeth, E; A pair of complementary demipyramids "dp" and "dp" are labeled on the face of the lantern closest to the viewer, F; enlarged image showing the keel and flange, while G; showing the details one of the five rotulae which separated each pair of complementary demipyramids. Scale bar = 1mm

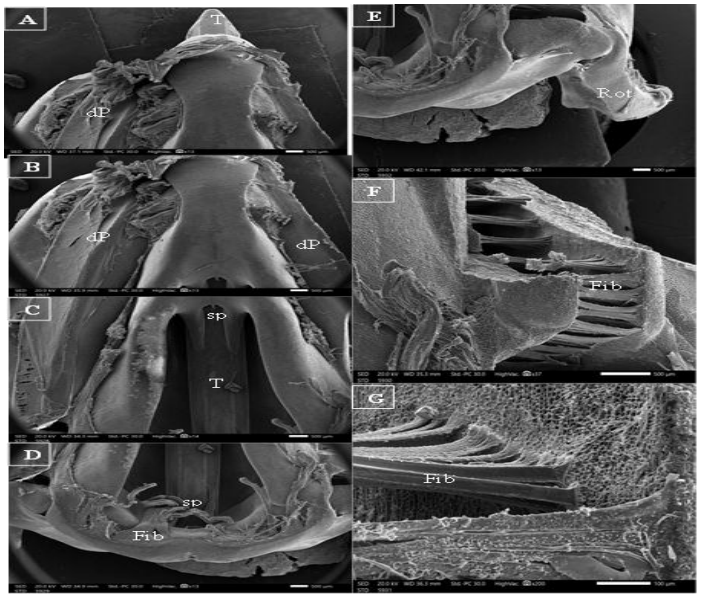

Figure 16: Scanning electron microscope image for different parts of *Echinometra mathaei* Aristole's lantern. (A) show the tooth shape (v) shape. (B) show the demipyramid structure from an internal view. (C) show the two demipyramid structures in addition to the upper two spines supporting the tooth. (D) show another two spines at lower part to support the tooth too and the fibers, which help in the attachment of the five teeth together and help in the connection with rotula and compass. (E) show the rotula structure. (F and G) show the fibers filaments that make a tight connection between thetooth lamella and demipyramid of the tooth. T= tooth, dp= demipyramid, sp= spines, Fib= Fibers, and Rot= Rotula. Scale bar= 500 µm

Figure 16 shows the microstructure of Aristotle's lantern in the species *E. mathaei*. The lantern consists of 40 skeletal components, including five teeth (Figures 15 A & 16 A), five rotulae (Figures 15 B, G & 16 E), ten hemi-pyramids (Figures 15 E & 16 A, B), ten epiphyses, and ten compass elements (Figure 15). Additionally, it contains various soft tissue structures, comprising numerous unpaired and paired muscle groups, according to recent research. Between each pair of pyramid

sections that support a tooth, there is a structure known as rotula, which serves separate them and connect them to a compass (Figures 15B, 15 G & 16 E).

Gonads:

E. mathaei has five lobes of gonads located within the perivascular coelom. Each gonad opens at a gonopore situated on a genital plate near the anus at the aboral end. The gonads are arranged around the aboral region of the coelom, with each one positioned in the center of its respective interambulacral area. They are surrounded by a translucent peritoneum, which is attached to the inner walls of the test by several slender supporting ligaments (Figure 17).

Water vascular system

The madreporite serves as the starting point for the water vascular system of the body (Figure 12 B). It leads into a stone canal that connects to an oval-shaped axial organ. The ring canal, also referred to as the water ring, is where the short, transparent stone canal ends (Figure 17) and originates on one side of the madreporite. There are five radial canals surrounding the mouth that extend from the ring canal. These canals lead to an ambulacrum, which connects to the ampulla, ultimately reaching the tube feet, also known as podia (Figure, 17).

Figure 17: Photograph illustrates the structure of the gonads and part of water vascular system. The madreporite acts as the entry point for this system, leading to the tube feet. The section of the madreporite that connects to the ring canal is where the axial organ develops. From the ring canal, five radial canals branch off into water canals, creating paired ampullae that extend as tube feet into the surrounding area. Scale bar = 10 mm.

3.3.Histology of internal organs: Peristome:

The peristome is made up of two main layers: a thick, multi-layered outer surface referred to as the "lip" and a deeper layer of connective tissue. Embedded within the lips are medium-sized cells that feature densely basophilic nuclei and cytoplasm that is moderately eosinophilic (Figure 18 A).

3.3.1. Peritoneal (coelomic) membrane:

The outer layer of the peritoneum is made up of closely aligned parallel units. Each unit features a large cell characterized by a prominently basophilic nucleus. Additionally, there are two types of fibroblast-like cells within each unit, distinguished by their elongated nuclei and highly eosinophilic cytoplasm, as well as two types of

globular cells that have either dense or transparent nucleoli. Observations revealed dense filamentous structures extending alongside the internal epithelial cells. These epithelial cells are positioned on the inner surface of the peritoneum (Figure 18 B). Toward the upper region of this epithelial layer, various cells are interconnected in a parallel arrangement, appearing to protrude into the coelomic cavity. These cells are reminiscent of certain coelomocytes.

3.3.2. Podium (tube foot):

The cross-section of the tube foot features a layer of basophilic epithelium extending from the lumen to the outer boundary. Within this structure, there are elongated muscle fibers arranged in bundles that resemble flagella and are highly eosinophilic. Additionally, a moderately eosinophilic layer of connective tissue is present, along with a dense layer consisting of neural cells that have very basophilic nuclei and eosinophilic cytoplasm. Finally, there are multiple rows of epithelial cells, as shown in (Figure 18 C).

3.3.3. Ampulla:

The cross-section of the tube foot features a basophilic epithelial layer extending from the lumen to the outer surface. It includes elongated muscles that are structured in bundles similar to flagella and are notably eosinophilic. There is also a moderately eosinophilic layer of connective tissue and a dense layer containing neural cells, which possess highly basophilic nuclei and eosinophilic cytoplasm. Lastly, several rows of epithelial cells are present (Figure 18 D).

3.3.4. Esophagus:

The esophagus is made up of several layers, including a mucus layer, a submucosal layer, connective tissue, and a muscle layer. The mucosal tissue features numerous cells with densely stained basophilic nuclei dispersed throughout a pink connective tissue backdrop. Parallel projections extend from this layer into the lumen in an organized manner.

The clusters of cells were located next to each other, separated by open spaces. Each cluster within the appendix contained many tightly packed cells, characterized by intensely basophilic nuclei and highly eosinophilic cytoplasm. The submucosal layer was not clearly identifiable. The inner layers comprised both connective and muscular tissues (Figure 18 E).

3.3.5. Stomach:

The histological structure of the stomach was similar to that of the esophagus, with the exception of cluster appendices in the mucosa that resembled parallel columnar villi. The entire surface was covered by epithelial cells that formed a distinct outer layer. These cells had nuclei that were moderately basophilic and cytoplasm that was moderately eosinophilic. Marginal cells in the submucosal layer appeared to act as a boundary between the mucosa and the submucosa. This layer contained fibroblast-like and parenchymal cells, which had larger, dense basophilic nuclei and a more eosinophilic quality compared to the cells in the surface layer (Figure 18 F).

3.3.6. Intestines:

The histological structure of the intestine resembles that of the stomach. The lumen features, narrow, columnar villi. Each villus consists of two types of cells in its mucosal layer.

The outer layer contains small cells with dense, slightly basophilic euchromatin nuclei, which house several small, dense, basophilic nucleoli, and have moderately eosinophilic cytoplasm. This layer is adjacent to a marginal cell layer from the submucosal zone, composed of larger cells with very basophilic, prominent nuclei and relatively small eosinophilic cytoplasm. In the inner part of the submucosa, fibroblast-like cells are arranged in parallel at the center. These cells exhibit elongated, moderately basophilic nuclei and large, moderately eosinophilic cytoplasm (Figure 18 G).

4. DISCUSSION

Characterization studies of certain echinoids, such as the red (*Strongylocentrotus franciscanus*), green (*S. droebachiensis*), and *Paracentrotus lividus* sea urchin (Amarowicz *et al*. 2012; Arizza *et al*., 2007), have been conducted in an incomplete and fragmented manner.

However, there has been no comprehensive study focusing on the anatomy, histology, and cytology of *E. mathaei* in the Red Sea. Six years prior, Zeina *et al*. (2016) identified 16 species of regular echinoids, which can be classified into 13 genera spanning 6 families and 4 orders. This study specifically focused on *E. mathaei*, a species previously examined by Hellal *et al*. (1995) and Zeina *et al*. (2016). In the present research, *E. mathaei* was identified through morphological analysis, aligning with the classification established by Zeina *et al*. (2016). Our objective was to characterize the Red Sea population of *E. mathaei* by investigating its surface morphology, anatomical structure, and histological features of both external and internal organs, as well as performing microscopy on coelomocytes to assess their surface and internal morphology. *E. mathaei* exhibits considerable diversity in test and spine morphology, alongside variations in coloration and shape, as noted by Arakaki *et al*. (1998) and Piryaei *et al*. (2018). The specimens we examined correspond to the morphological traits previously documented for *E. mathaei*. The organism displays radial symmetry, with its body parts organized in quintets. Radially symmetrical organisms possess a distinct top and bottom but do not exhibit clear left and right or front and back orientations.

Species characterized by penta-radial symmetry can typically navigate in any direction with ease, a phenomenon referred to as omnidirectional movement, as discussed by Morrissey and Sumich (2012) and Piryaei *et al*. (2018).

The body surface is rigid and robust due to the underlying test, which also provides an attachment point for the sea urchin's spines (Drozdov *et al*., 2016). Our observations revealed two distinct test shapes: at the first study site, the shell was more compressed and oval, while at the second site, it appeared more spherical.This variation in test morphology may be attributed to the differing habitats and depths from which the specimens were collected. In our analysis, we categorized spines into two distinct types based on their tips, which were either blunt or sharp. The spines with blunt tips exhibited a softer texture and a pinkish hue, and their specific function remains ambiguous, necessitating further histological studies. The spine dimensions and sharpness vary among species, with the genus *Diadema* having the longest spines compared to *E. mathaei*. (Nour *et al*., 2022). Certain species possess sharp spines that provide protection against predators.

Additionally, we observed that the spines exhibit multidirectional movement and serve as a primary defense mechanism for sea urchins. This research represents the inaugural effort to classify spines into seven categories based on size, corroborating the findings of (Piryaei *et al*., 2018).

The pedicellariae of sea urchins function as biting jaws and serve as a secondary line of defense (Moitoza and Phillips, 1979). Four distinct types of pedicellariae exhibit varied directional movements and continuously open and close their sharp prongs. Our results corroborate the findings of Moitoza and Phillips (1979) as well as Piryaei *et al*. (2018). The globiferous pedicellariae found in E. mathaei bear a close resemblance to those characterized by Campbell in 1983, which were identified as venomous structures (Coppard and Campbell, 2006).

Given this notable morphological similarity, it is plausible that the globiferous pedicellariae in *E. mathaei* may harbor venomous compounds. Additional research is warranted to further investigate this hypothesis (Newton and Dennis, 2021).

The oral side of the test displays a significant opening known as the mouth, which is surrounded by a flexible membrane called the peristome. This peristome is vital to the structural framework of the lantern in regular echinoids (Bonasoro *et al*., 1995). Our findings correspond with studies on other echinoids, such as *Paracentrotus lividus*, where the teeth and adjacent layers resemble those of *E. mathaei* (Bonasoro *et al*., 1995). An ultrastructural examination of the Aristotle lantern showed that the teeth have a V-shape. In cidaroids, tooth tips can vary in shape, including crescent and V configurations (Ziegler *et al*., 2012). Our histological study of the peristome highlights its functional versatility in regular sea urchins, showcasing the remarkable properties of its connective tissue, which is identified as variably collagenous (Wilkie *et al*., 2004; Tricarico, 2013; Piryaei *et al*., 2018). *E. mathaei*, similar to other sea urchin species, has a specialized jaw structure that allows for effective algae consumption. This may be a result of their similar diets that require the ability to crush both soft and hard food types. *E. mathaei* is well-known for its algal diet, as noted by Nagai and Kaneko (1975) and Cook and Kelly (2007).The present work we revealed that there was differences in *E. mathaei* tube feet ossicles structure collected from the two study sites. These differences may reflect environmental adaptation or genetic divergence. Chadwick (1900) and Stott (1955) provided insights into the anatomy and histology of the food canal in regular echinoids. Despite *E. mathaei's* prevalence in subtidal zones across global oceans, comprehensive anatomical and histological studies of its digestive system have been limited. Piryaei *et al*. (2018) offered detailed descriptions of the food canal and its associated hemal canals in *E. mathaei* found in the Persian Gulf. Histologically, the food canal wall comprises an outer epithelial layer, circular and longitudinal muscle layers, varying thicknesses of connective tissue, and an inner epithelium made up chiefly of tall, slender cells (Piryaei *et al*., 2018). The histological aspects of the food canal in *E. mathaei* correspond with Piryaei's observations.Campos-Creasey (1992) indicated that the esophageal wall in *Echinus esculentus* is primarily composed of a uniform layer of tall, slender, cylindrical mucus-producing cells. These findings align with those in *E. mathaei*.

The stomach lining of *Strongylocentrotus intermedius* consists of groups of elongated columnar cells filled with small granules (De Ridder and Jangoux, 2020.). These granules are found only in the stomach lining, while *E. mathaei* does not present similar structures. The stomach histology of *E. mathaei* shows parallels to that of *S. intermedius*.

The histo-morphological characteristics of the food canal in *E. mathaei* described by Piryaei *et al*. (2018) from the Persian Gulf align with our findings from the Red Sea.

Additionally, Boolootian's (1964) research on the histo-morphological structure of the food canal in *S. intermedius* confirms our observations in *E. mathaei*. Research on nutrient transfer between the gut and other organs remains limited, although studies by Farmanearmaian and Pmllivs (1962), Giese *et al*. (1959), Greenfield *et al*. (1958), and Stott (1955) suggested that coelomic fluid might facilitate this process. Tube feet, essential elements of the echinoderm water-vascular system, exhibit varied forms and functions (Flammang, 1996). Steen (1965) proposed that these fleshy, tubular structures are connected to the hydrovascular system, playing roles in the movement, respiration, and sensory functions. Research by Lesser *et al*. (2011) found that the terminal portion of the tube feet in the green sea urchin (*S. droebachiensis*) comprises five ossicles arranged to capture light, with their concave sides facing light sources. This newly discovered function adds to the recognized roles of tube feet. The anatomical features of these structures are similar to those in other echinoderms,

including *P. lividus* and *M. glacialis*. Each tubular leg ends in a disc that aids in attachment and sensory functions.

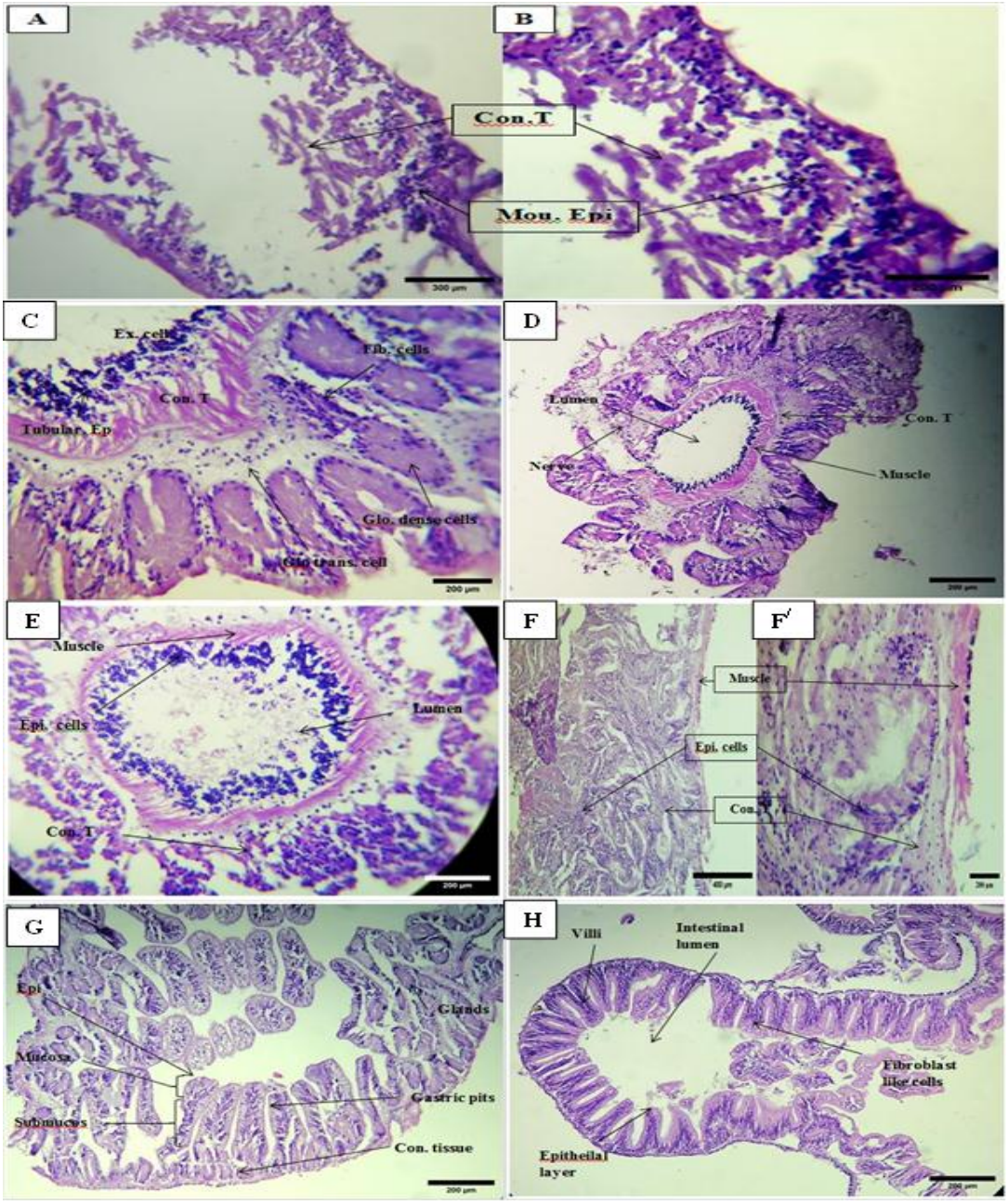

Figure 18: Histological sections of *Echinometra mathaei* internal organs. (A & B). Peristome. (C) Peritoneal membrane. (D) Tube feet. (E) Ampoule. (F & F/) Esophagus. (G) Stomach. (H) Intestine. Scale bar (A= 300 µm, B, C, D, E , F/ , G & H = 200 µm, and F = 400 µm).

Our observations showed that aboral tube feet can move in various directions, much like sensory organs seeking stimuli. It was observed that the oral tube feet of the sea urchin can stick to the glass walls of the aquarium as the sea urchin moves. The muscular layer within the tube feet is crucial for their movement.

The water-vascular system connects to these tube feet and includes a central pore that acts as a vacuum, allowing the sea urchin to hold tightly onto vertical surfaces. The differences between the aboral and oral tube feet indicate that they serve distinct roles. Additionally, tube feet may provide valuable functions.

CONCLUSION

This research examines the anatomy and histology of *Echinometra mathaei*, highlighting key differences that distinguish this species. A notable variation in ossicle morphology was observed between two study sites, with one site showing irregular perforations and the other more uniform structures.

Detailed analysis of the lantern revealed its five-fold symmetry, complex muscle arrangements, and rotulae, providing insights into its biomechanics and food processing role. The spines' stereom was described in detail, emphasizing micro-perforation patterns and semi-circular spicules as diagnostic features.

ACKNOWLEDGMENT

Authors would like to thank Marine Genomics Unit, Faculty of Science, Benha University, Egypt for providing the necessary resources, facilities, and an enriching academic environment that were crucial to the successful completion of this research. The department's support has been instrumental in this research.

REFERENCES:

Amarowicz, R., Synowiecki, J. & Shahidi, F. 2012. Chemical composition of shells from red (*Strongylocentrotus franciscanus*) and green (*Strongylocentrotus droebachiensis*) sea urchin. Food Chemistry, 133(3), 822-826. doi.org/10.1016/j.foodchem.2012.01.099.

Arakaki, Y., Uehara, T., & Fagoonee, I. 1998. Comparative studies of the genus Echinometra from Okinawa and Mauritius. *Zoological Science*, *15*(1), 159-168. doi.org/10.2108/zsj.15.159

Arizza, V., Giaramita, F. T., Parrinello, D., Cammarata, M. & Parrinello, N. 2007. Cell cooperation in coelomocyte cytotoxic activity of *Paracentrotus lividus* coelomocytes. *Comparative Biochemistry and Physiology Part A: Molecular &* Integrative Physiology, 147(2), 389-94. doi.org/10.1016/j.cbpa.2007.01.022

Ball, B., & Jangoux, M. 1990. Ultrastructure of the tube foot sensory-secretory complex in *Ophiocomina nigra* (Echinodermata, Ophiuridea). *Zoomorphology*, *109*, 201-209. doi.org/10.1007/BF00312471

Bonasoro, F., Candia, D. & Wilkie, C. 1995. The peristomial membrane of regular sea-urchins: functional morphology of the epidermis and coelomic lining in *Paracentrotus lividus* (Lamarck). *Italian Journal of Zoology*, 62(2), 121-135. doi.org/10.1080/11250009509356060

Boolootian, R. & Lasker, R. 1964. Digestion of brown algae and the distribution of nutrients in the purple sea urchin *Strongylocentrotus purpuratus*. *Comparative Biochemistry and Physiology*, *11*(3), 273-289. doi.org/10.1016/0010-406X(64)90109-4

Campbell, A. C. 1983. Form and function of pedicellariae. *Echinoderm Studies* 1, 139–167.

Campbell, A. C. 1987. Echinoderms of the Red Sea. *Red Sea (eds. Edwards, AJ, Head, SM)*, 215-232.

Campos-Creasey, L.1992. A study of the feeding biology of deep-sea echinoids from the North Atlantic. (PhD) University of Southampton.

Cavey, M. & Märkel, K. 1994. Echinodermata. Microscopic Anatomy of Invertebrates, 2nd Ed., *Wiley-Liss*, 345-400.

Chadwick, H. C. 1900. Echinus. Proceedings and Transactions of the Liverpool Biological Society. 14 Memoirs, 3: 1–28.

Cook, E. J., & Kelly, M. S. 2007. Enhanced production of the sea urchin *Paracentrotus lividus* in integrated open-water cultivation with Atlantic salmon *Salmo salar*. *Aquaculture*, *273*(4), 573-585. doi.org/10.1016/j.aquaculture.2007.10.038

Coppard, S. & Campbell, A. 2006. Systematic significance of tridentate pedicellariae in the echinoid genera Diadema and Echinothrix. *Invertebrate Biol.*, *125*(4),363-378. doi.org/10.1111/j.1744-7410.2006.00068.x

Drozdov, A., Sharmankina, V. Zemnukhova, L.& Polyakova, N.2016. Chemical composition of spines and tests of sea urchins. *Biology Bulletin*, *43*, 521-531. doi.org/10.1134/S1062359016060078

Farmanearmaian, A., & Pmllivs, J. 1962. Digestion, storage, and translocation of nutrients in the purple sea urchin, *Strongylocentrotus purpuratus*. *Biology Bulletin*, 123, 105-120. doi.org/10.2307/1539507

Fielding, J., Hallissey, M., Daniels, I. & Allum, W. (2005). The anatomy and physiology of the stomach. *Upper gastrointestinal surgery*, 17-37.

Flammang, P. 1996. Adhesion in echinoderms. *In Echinoderm Studies*, Vol. 5 (ed. M. Jangoux and J. M. Lawrence), Rotterdam: Balkema, pp. 1-60.

Giese, A. Greenfield, L., Huang, H., Farmanfarmaian, A., Boolootian, R. & Lasker, R. 1959. Organic productivity in the reproductive cycle of the purple sea urchin. *Biology Bulletin*, 116, 49-58. doi.org/10.2307/1539155

Greenfield, L., Giese, A.C., Farmanfarmaian, A. & Boolootian, R A.1958. Cyclic biochemical changes in several Echinoderms. *Journal of Experimental Zoolog*, 139, 507-524. doi.org/10.1002/jez.1401390308

Großmann, J. N. 2010. Stereom differentiation in sea urchin spines under special consideration as a model for a new impact protective system (PhD), Universität Tübingen. hdl.handle.net/10900/49467

Hellal, A. M., Abou-zeid, M, & El-Sayed, A. A. M. 1995. Final Report on MacroInvertebrate Fauna at Protected Areas of South Sinai. EEAA, pp115.

Lesser, M. P., Carleton, K. L., Böttger, S. A., Barry, T. M. & Walker, C. W. 2011. Sea urchin tube feet are photosensory organs that express a rhabdomeric-like opsin and PAX6. *Proceedings. Biological sciences*, 278, 3371–3379. doi.org/10.1098/rspb.2011.0336

Märkel, K., & Röser, U. 1983. The spine tissues in the echinoid (*E. tribuloides*). *Zoomorphology* 103:25–41. doi.org/10.1007/BF00312056

Moitoza, D. J. & Phillips, D. 1979. Prey defense, predator preference, and nonrandom diet: The interactions between *Pycnopodia helianthoides* and two species of sea urchins. *Marine Biology*, 53, 299-304. doi.org/10.1007/BF00391611

Morrissey, J. F., & Sumich, J. L. 2012. Introduction to the Biology of Marine Life (10th Edition). Jones & Bartlett Learning, pp. 467.

Moureaux, C., & Dubois, P. 2012. Plasticity of biometrical and mechanical properties of Echinocardium cordatum spines according to environment. *Marine biology*, *159*, 471-479. doi.org/10.1007/s00227-011-1824-2

Nagai, Y., & Kaneko, K. 1975. Culture experiments on the sea urchin *S. pulcherrimus*

fed an artificial diet. *Marine Biology*, *29*(2), 105-108. doi.org/10.1007/BF00388981

Newton, A. L., & Dennis, M. M. 2021. Echinodermata. *Invertebrate histology*, 1-18. doi.org/10.1002/9781119507697.ch1

Nour, O. M., Al Mabruk, S. A., Adel, M., Corsini-Foka, M., Zava, B., Deidun, A., & Gianguzza, P. 2022. First occurrence of the needle-spined urchin *Diadema setosum* (Leske, 1778) (Echinodermata, Diadematidae) in the southern Mediterranean Sea. www.um.edu.mt/library/oar/handle/123456789/89841

Piryaei F., Ghavam M, P., Shahbazzadeh, D. & Pooshang Bagheri, K. 2018. Description on anatomy and histology of Echinometra mathaei (Echinoidea: Camarodonta: Echinometidae), the Persian Gulf sea urchin. *Sustainable Aquaculture & Health Management J*, *4*:1-27. dx.doi.org/10.29252/ijaah.4.2.1

Prabhu, H., Lakshmipathi, M., Temesgen, B., & Habte, F. 2015. Spatial and temporal distribution of sea urchins in the coastal waters of Massawa, Eritrea. *Journal of Academia and Industrial Research*, *3*(10), 472-478.

Price, A. G. 1983. Fauna of Saudi Arabia, Echinoderms of Saudi Arabia, Echinoderms of the Persian Gulf coast of Saudi Arabia pp, 29-109.

Price, A. G. 1986. A field guide to the sea shores of Kuwait and the Persian Gulf, Phylum Echinodermata. *Blandfo press* pp, 136-143.

Rashad, M., Shaban, W.M., Ali, A.H.& Abdel-Salam, H. 2020. Reproductive traits and Microstructure of *Acropora digitifera* and *Acropora gemmifera* (Scleractinia, Anthozoa) inhabiting the Northern Red Sea (Hurghada, Egypt). *Egyptian. J. Aquatic Biol. and Fish.*, 24(4) 249-266. DOI: 10.21608/ejabf.2020.97537

Ruppert, E., Richard, F. S., & Barnes, R. D. 2004. Invertebrate Zoology, 7th edition. Cengage Learning. pp. 896–906.

Steen, J. B. 1965. Comparative Aspects of the Respiratory Gas Exchange of Sea Urchins. *Acta Physiologica*, 63, 161-1. doi.org/10.1111/j.1748-1716.1965.tb04054.x

Stott, F. C. 1955. The food canal of the Sea-urchin *Echinus esculentus* L. and its functions. In *Proceedings of the Zoological Society of London* (Vol. 125, No. 1, pp. 63-86). Oxford, UK: Blackwell Publishing Ltd. doi.org/10.1111/j.1096-3642.1955.tb00592.x

Strathmann, R. 1981. The role of spines in preventing structural damage to echinoid tests. *Paleobiology*, *7*(3), 400-406.

Tricarico, S. 2013. Biology of the dynamic connective tissue (MCTs) in invertebrate marine models: an integrated approach. oordinatore: M. Ferraguti. Universita' degli studi di Milano, ciclo, Anno Accademico. [10.13130/tricarico-serena_phd2013-01-24]. hdl.handle.net/2434/215687

Wilkie, I., McKew, M. & Carnevali, M. 2004. Unusual morphological features of the compass-rotular ligament of *Echinus esculentu* L. In *Echinoderms: Munchen: Proceedings of the 11th International Echinoderm Conference, 6-10 October 2003, Munich, Germany* (p. 379). Taylor & Francis. hdl.handle.net/2434/178724

Zeina, A. F., Darweesh, K. F., & Hellal, A. M. 2016. Sea urchins (Echinoidea: Echinodermata) from Gulf of Aqaba, Red Sea, Egypt. *Int. J. Develop.*, *5*(1), 129-147. www.%20ijd.byethost13.com

Ziegler, A., Schröder, L., Ogurreck, M., Faber, C. & Stach, T. 2012. Evolution of a novel muscle design in sea urchins (*Echinoidea*). *PloS one*, *7*(5), e37520. doi.org/10.1371/journal.pone.0037520